Carbohydrate Polymers 94 (2013) 199–208

Contents lists available at SciVerse ScienceDirect

Carbohydrate Polymers

journal homepage: www.elsevier.com/locate/carbpol

Physical–mechanical and antimicrobial properties of nanocomposite films with pediocin and ZnO nanoparticles

Paula Judith Perez Espitia[a], Nilda de Fátima Ferreira Soares[a,*], Reinaldo F. Teófilo[b], Jane Sélia dos Reis Coimbra[a], Débora M. Vitor[a], Rejane Andrade Batista[a], Sukarno Olavo Ferreira[c], Nélio José de Andrade[a], Eber Antonio Alves Medeiros[a]

[a] Food Technology Department, Federal University of Viçosa, Av. P. H. Rolfs s/n, Campus Universitário, 36570-000 Viçosa, Minas Gerais, Brazil
[b] Department of Chemistry, Federal University of Viçosa, Av. P. H. Rolfs s/n, Campus Universitário, 36570-000 Viçosa, Minas Gerais, Brazil
[c] Department of Physics, Federal University of Viçosa, Av. P. H. Rolfs s/n, Campus Universitário, 36570-000 Viçosa, Minas Gerais, Brazil

ARTICLE INFO

Article history:
Received 5 November 2012
Received in revised form
21 December 2012
Accepted 1 January 2013
Available online 10 January 2013

Keywords:
ZnO nanoparticles
Pediocin
Food packaging
Nanocomposite films
Food preservation
Food borne pathogens
Packaging characterization

ABSTRACT

This work aimed to develop nanocomposite films of methyl cellulose (MC) incorporated with pediocin and zinc oxide nanoparticles (nanoZnO) using the central composite design and response surface methodology. This study evaluated film physical–mechanical properties, including crystallography by X-ray diffraction, mechanical resistance, swelling and color properties, microscopy characterization, thermal stability, as well as antimicrobial activity against *Staphylococcus aureus* and *Listeria monocytogenes*. NanoZnO and pediocin affected the crystallinity of MC. Load at break and tensile strength at break did not differ among films. NanoZnO and pediocin significantly affected the elongation at break. Pediocin produced yellowish films, but nano ZnO balanced this effect, resulting in a whitish coloration. Nano ZnO exhibited good intercalation in MC and the addition of pediocin in high concentrations resulted crater-like pits in the film surfaces. Swelling of films diminished significantly compared to control. Higher concentrations of Nano ZnO resulted in enhanced thermal stability. Nanocomposite films presented antimicrobial activity against tested microorganisms.

1. Introduction

World use of plastics has increased enormously, compounding the problem of waste contamination. In the United States alone, increased plastic production resulted in 31 million tons of plastic waste in 2010, representing 12.4% of total Municipal Solid Waste (MSW)—commonly known as trash or garbage (EPA, 2011). As plastic products continue to increase, they bring a number of environmental concerns. Such concerns have created increased interest in biopolymers research, due to their biodegradability.

Methyl cellulose (MC) has become an attractive alternative, due its ability to allow the development of environmental friendly products, its large availability in nature, low cost and easy processing. This biodegradable carbohydrate polymer is a modified type of cellulose and is the most abundant biopolymer in nature (Rimdusit, Jingjid, Damrongsakkul, Tiptipakorn, & Takeichi, 2008).

However, biodegradable natural packaging materials usually have poor mechanical, barrier and thermal characteristics (Tunç & Duman, 2011).

Research has shown that new materials with improved properties can be developed using nanotechnology. These new materials are known as nanocomposites, which are hybrid materials where the filler incorporated in the polymeric matrix has at least one dimension in the nanometer scale (Espitia et al., 2012).

Polymer/clay nanocomposites have been one of the most widely studied nanocomposites and research has shown that the developed nanocomposites often exhibit enhanced thermal stability, physical–mechanical and barrier properties compared to neat polymer matrix (Arora & Padua, 2010). However, studies dealing with nanocomposites of MC are scarce, and few have focused on the application of biopolymer nanocomposites as active packaging materials for food preservation (Lagarón & Fendler, 2009).

Antimicrobial packaging is a type of active packaging which interacts with the product or the headspace inside to reduce, inhibit or retard the growth of microorganisms that may be present on food surfaces (Soares et al., 2009). In order to develop nanocomposite films for antimicrobial food packaging, zinc oxide (ZnO) nanoparticles and pediocin were incorporated into the MC matrix.

* Corresponding author. Tel.: +55 31 38992020; fax: +55 31 38992208.
E-mail addresses: nfsoares10@gmail.com, nfsoares@ufv.br (N.d.F.F. Soares).

0144-8617/$ – see front matter © 2013 Elsevier Ltd. All rights reserved.
http://dx.doi.org/10.1016/j.carbpol.2013.01.003

Table 1
Coded (in brackets) and decoded levels of ZnO nanoparticles and pediocin concentration for the CCD.

Treatment codification[a] (TRT)	ZnO nanoparticles (% w/w)	Pediocin (% w/w)
	Uncoded	Uncoded
8	11.0 (0)	50 (+1.41)
6	19.5 (+1.41)	33 (0)
3	5.0 (−1)	45 (+1)
11c	11.0 (0)	33 (0)
5	2.5 (−1.41)	33 (0)
10c	11.0 (0)	33 (0)
7	11.0 (0)	15 (−1.41)
1	5.0 (−1)	20 (−1)
13c	11.0 (0)	33 (0)
4	17.0 (1)	45 (+1)
9c	11.0 (0)	33 (0)
12c	11.0 (0)	33 (0)
2	17.0 (+1)	20 (−1)

[a]c in the central point. Coded levels are in parenthesis.

ZnO is an inorganic compound widely used in everyday applications, is currently listed as a generally recognized as safe (GRAS) material by the Food and Drug Administration (21CFR182.8991) and has previously shown antimicrobial activity against food borne pathogens (Espitia et al., 2012; FDA, 2011).

Moreover, pediocin is a bacteriocin, also considered a bioactive peptide, which is ribosomally synthesized by *Pediococcus acidilactici* and has the ability to kill closely related bacteria. Pediocin has many applications in food preservation due to its activity in controlling *L. monocytogenes*, a food borne pathogen of special concern in the food industry (Rodríguez, Martínez, & Kok, 2002).

Therefore, this work aimed to develop nanocomposite films incorporated with pediocin and ZnO nanoparticles. Also this work aimed to evaluate physical–mechanical properties, including microscopy analysis, tensile test, color properties and thermal stability, as well as antimicrobial activity against *S. aureus* and *L. monocytogenes* of developed nanocomposite films using the central composite design and statistical approaches of response surface methodology (RSM).

2. Materials and methods

2.1. Materials

Methyl cellulose (MC) and zinc oxide (ZnO) nanoparticles were purchased from Sigma–Aldrich Chemical Co. (USA). Pediocin was purchased in the form of a commercially available concentrate known as ALTA™ 2341 (Kerry Bioscience, Ireland). Also, sodium pyrophosphate ($Na_4P_2O_7$) at 0.1 M was purchased from Sigma–Aldrich Chemical Co., (USA) and used as the dispersing agent of ZnO nanoparticles. Glycerol (Labsynth, Sao Paulo, Brazil) was used as a film plasticizer.

2.2. Film production

For film production, ZnO nanoparticles were dispersed according to the following procedure: Different concentrations of ZnO nanoparticles (Table 1) were mixed with 150 mL of deionized water (Millipore Milli-Q system) and 0.1 M sodium pyrophosphate (0.13 g) was added. The ZnO nanoparticle dispersion process was done in a probe sonicator (DES500 Unique, Brazil) with a 1.1 cm diameter probe. ZnO nanoparticles were sonicated using 200 W of power for 23 min. After ZnO dispersion, glycerol (0.8 g) was added to the nanoparticle solution, which was heated at 80 ± 2 °C to solubilize the polymer (methyl cellulose). Pediocin was added to the nanoparticle solution at different concentrations according to the central composite design (item 2.3) and with MC (7.5 g) in order to obtain the filmogenic solution. The filmogenic solution was cast in cubic molds made from glass, with inner dimensions of 18 × 34 cm^2. Casted nanocomposite films were dried for 72 h at ambient conditions (18 °C and 65% RH).

2.3. Experimental design and statistical analysis

A central composite design (CCD) was used to study the combined effects of ZnO nanoparticles and pediocin on the engineering properties and antimicrobial activity of MC nanocomposite films. The experiment was carried out according to a CCD based on the Response Surface Methodology (RSM), with two variables (Table 1): concentration of ZnO nanoparticles and pediocin in the filmogenic solution (each antimicrobial concentration was based on MC dry weight).

A statistical model representing the influence of ZnO nanoparticles and pediocin on the engineering properties and antimicrobial activity of nanocomposite film was developed and validated using the analysis of variance (ANOVA). Treatment effects on response were assessed by RSM. All calculations and graphics in this work were performed using electronic worksheets from Microsoft® Excel 2003 according to Teófilo and Ferreira (2006).

2.4. Optimization by the desirability function approach

After the elaboration of response surface models, a simultaneous optimization of significant response variables was done using the desirability function approach according to Derringer and Suich (1980). Each estimated response variable, calculated by the fitted response surface associated with the CCD experimental design used in this work, was transformed using the desirability function into a desirable value (d_i), using the following equation:

$$d_i = \begin{cases} 0 & \hat{y}_i \le y_{i\min} \\ \left[\dfrac{\hat{y}_i - y_{i\min}}{y_{i\max} - y_{i\min}}\right] & y_{i\min} < \hat{y}_i < y_{i\max} \\ 1 & \hat{y}_i \ge y_{imax} \end{cases} \quad (1)$$

where the values y_{imin} and y_{imax} are the minimum and maximum acceptable value of $\hat{y}_i$, respectively. The values of d_i vary in the interval $0 \le d_i \le 1$, increasing as the desirability of the corresponding response increases. The individual desirabilities were then combined using the geometric mean (Eq. (2)) to give an overall desirability (D).

$$D = (d_1 \times d_2 \times \cdots \times d_k)^{1/k} \quad (2)$$

The overall desirability was analyzed using a univariate search technique to optimize D over the independent variable domain, which resulted in the desirability of the combined response levels. In this work the desirability function varied between zero and one.

2.5. Film characterization

2.5.1. X-ray diffraction (XRD) characterization

The diffraction pattern was obtained to confirm the crystalline structure of ZnO nanoparticles alone, as well as incorporated in the nanocomposite films. XRD patterns were taken with the X-ray Diffraction System X'Pert PRO model (PANalytical, Netherland), using an iron (Fe) filter and Co K_α radiation (λ = 1.78890 Å). The diffraction pattern was obtained at diffraction angles between 10° and 80° (2θ).

2.5.2. Measurement of film thickness

Thickness of the samples was determined with a manual digital micrometer (0.01 mm, Mitutoyo Sul Americana, Suzano, São Paulo State, Brazil). The thickness of the nanocomposite films was measured at ten randomly selected points on each film to calculate the average value. Average values were used when necessary to calculate film properties.

2.5.3. Mechanical resistance

Mechanical properties of developed nanocomposite films (tensile strength at break, load at break and elongation at break) were determined according to the standard method ASTM D882-09 (ASTM, 2009) using an Instron Universal Testing Machine model 3367 (Instron Corporation, Norwood, MA, USA), equipped with a load cell of 1 kN. The nanocomposite film samples were cut in rectangular specimens ($15 \times 2.5\ cm^2$). Initial grip separation was 100 mm, and the cross-head speed was set at 50 mm/min. This test was repeated ten times for each treatment to confirm its repeatability.

2.5.4. Surface color measurement

Color values of films were measured with a colorimeter COLORQUEST XE HUNTERLAB (Reston, Virginia, USA). The instrument was used with a 9.5 mm diameter of measuring area. The measurements were done in the CIELAB scale, in which each measurement is expressed as L^* (indicating the lightness), a^* (positive in the red direction and negative in the green direction), and b^* (positive in the yellow direction and negative in the blue direction). Calculations were made for D-65 illuminant and 10° observation interval according to ASTM E308 (ASTM, 2008). Total color differences (ΔE) and opacity (OP) were calculated using the standard values of the white background ($L^* = 93.44$; $a^* = -0.63$; $b^* = 1.21$). Also, the yellowness index (YI E313) and whiteness index (WI E313) were obtained using the Universal Software V4.10 according to ASTM E313-10 (ASTM, 2010). All color measurements were repeated three times for each type of nanocomposite film.

2.5.5. Microscopy characterization

Morphological analyses of nanocomposite films were observed directly by Scanning Electron Microscopy (SEM, Hitachi-TM 3000 Tabletop microscope, Japan). The topography of nanocomposite films was studied using Atomic Force Microscopy (AFM, NT-MDT, Russia). AFM images were acquired in an intermittent contact mode in random areas of $50 \times 50\ \mu m^2$. The samples were analyzed in air at room temperature (25 °C).

2.5.6. Swelling tests

Swelling tests were done according to Jipa, Stoica-Guzun, and Stroescu (2012) with some modifications. Samples of nanocomposite films in triplicate ($2 \times 2\ cm^2$) were dried to constant weight, and immersed in distilled water at room temperature (25 °C) for 2 h. The polymer mass dissolved in distilled water was neglected considering the short time needed for the experiment. Also, the amount of both antimicrobial (ZnO nanoparticles and pediocin) incorporated in the active films and their released in aqueous media was considered negligible compared to the amount of absorbed water. Swelling degree was obtained by measuring the initial mass (m_i) and the mass of sample in swollen state (m_s) using Eq. (3):

$$SD = 100 \times \left(\frac{m_s - m_i}{m_i} \right) \quad (3)$$

The mass of swollen sample was measured after gently blotting film surface with tissue paper until the equilibrium was reached.

2.5.7. Thermogravimetric analysis

Analysis was performed on a thermogravimetric analyzer (TGA-1000, Navas instruments, Conway, SC, USA). Samples of nanocomposite film (1 g approx.) were heated to 950 °C, at a heating rate of 10 °C/min under nitrogen atmosphere. Weight losses of samples were measured as a function of temperature.

2.5.8. Microorganisms and antimicrobial activity assay

S. aureus (ATCC 6538) and *L. monocytogenes* (ATCC 15313) were used to test the antimicrobial activity of developed nanocomposite films. Bacteria stored at −80 °C, were grown twice in Tryptic Soy Broth (TSB; Acumedia, Baltimore MD, USA) and incubated for 24 h at 35 °C. Bacteria were streaked on non-selective culture media Tryptic Soy Agar (TSA; Acumedia, Baltimore MD, USA) and incubated for 24 h at 35 °C to isolate bacterial colonies. Isolated colonies were selected from the TSA Petri dish and suspended in saline solution (0.85%, w/v). The bacterial suspension was adjusted to achieve the turbidity of McFarland standard solution 0.5, resulting in an inoculum containing approximately 1×10^8 CFU/mL.

Bacterial inoculum of *S. aureus* was subcultured in Baird Parker Agar (Hi-Media Laboratories, Mumbai, India), while bacterial inoculum of *L. monocytogenes* was subcultured in Oxford agar (Difco Laboratories) for the antimicrobial activity assay.

Following this, discs (1 cm diameter) of each treatment of nanocomposite films were placed on the surface of the previously inoculated agar culture media. Petri dishes with microorganism and discs of nanocomposite films were incubated at 12 ± 1 °C for 24 h to allow the diffusion of antimicrobial compounds (pediocin and ZnO nanoparticles) from the films without microbial growth. Petri dishes were incubated at 35 ± 1 °C for 24 h.

The antimicrobial activity of nanocomposite films was determined by measuring the inhibition zone around each disc of films (cm). All samples were tested in triplicate.

3. Results and discussion

3.1. X-ray diffraction (XRD) characterization

The XRD technique uses the scattered intensity of an X-ray beam on the sample, revealing information about the crystallographic structure, chemical composition, and physical properties of the material studied. This technique is widely used in materials characterization since is nondestructive and does not require elaborated sample preparation (Espitia et al., 2012).

Pure ZnO nanoparticles, film of neat MC and nancomposite films were analyzed using XRD technique (Fig. 1). In this work we report the results obtained for nancomposite films regarding treatments TRT6 and TRT8, since these treatments present the maximum tested levels of ZnO nanoparticles and pediocin. Moreover, the calculated interplanar spacing (d) of ZnO nanoparticles matched with the standard (JCPDS N°. 036-1451), confirming the hexagonal wurtzite structure of ZnO nanoparticles.

These results showed main characteristic peaks of ZnO nanoparticles (observed at $2\theta = 37.2°$; $2\theta = 40.3°$; $2\theta = 42.5°$; $2\theta = 55.9°$), confirming that the hexagonal wurtzite structure of ZnO nanoparticles was not affected after their incorporation in MC matrix. Moreover, the intensity of main characteristic peaks of ZnO was higher as the concentration of ZnO nanoparticles in MC matrix increased.

For the film of neat MC, main diffraction peaks were observed at $2\theta = 9.1°$, $2\theta = 15.6°$, and a broad peak around $2\theta = 25°$, which represent its partial crystallinity structure. According to Espinoza-Herrera, Pedroza-Islas, San Martín-Martinez, Cruz-Orea, and Tomás (2011), MC has a high proportion of amorphous structure and a natural partial crystallinity.

Table 2
Estimated regression coefficients for the elongation at break (%) and colorimetric parameters of nanocomposite films incorporated with ZnO nanoparticles and pediocin.

Independent variable[a]		Elongation at break	Colorimetric parameter					
			L^*	b^*	OP	ΔE	WI E313	YI E313
Mean		***34.72***	***90.49***	***11.08***	***55.28***	***9.627***	***24.71***	***19.67***
ZnO		***−3.985***	0.251	***−0.259***	***11.32***	***−0.331***	***1.936***	−0.283
PED		***5.716***	***−0.942***	***2.416***	***1.282***	***2.27***	***−13.58***	***4.418***
ZnO^2		***4.781***	−0.055	−0.044	***−3.291***	−0.005	−0.093	−0.058
PED^2		1.605	−0.134	0.001	0.819	0.023	0.009	−0.053
ZnO × PED		−4.269	−0.17	−0.11	0.5	−0.014	0.096	−0.111
Regression	F[b]	11.27	9.366	31.2	162.7	27.21	29.65	38.12
	P[c]	0.003044	0.005246	0.000121	$4.4{\cdot}10^{-07}$	0.00019	0.000143	$6.23{\cdot}10^{-05}$
Lack of fit	F[b]	0.895	1.59	11.22	2.203	15.28	12.76	13.01
	P[c]	0.517008	0.324352	0.020388	0.230201	0.011755	0.016248	0.015697

[a] ZnO, linear effect of ZnO nanoparticles; PED, linear effect of pediocin; ZnO^2, quadratic effect of ZnO nanoparticles; PED^2, quadratic effect of pediocin; ZnO × PED, effect of the interaction of ZnO nanoparticles and pediocin. Values in bold and italics are significant at $\alpha = 0.05$ with 4 degrees of freedom for the response variable.
[b] F distribution.
[c] p-Value.

Moreover, as observed in the XRD patterns of nanocomposite films, the addition of ZnO nanoparticles and pediocin affected the crystallinity of MC matrix. In this way, the addition of ZnO nanoparticles resulted in narrow peaks of MC, indicating more crystallinity structure of films; on the other hand, higher concentrations of pediocin resulted in broader peaks, mainly observed in XRD pattern of TRT8, indicating that the addition of pediocin resulted in lower crystallinity.

3.2. Thickness and mechanical resistance of nanocomposite films

Results of thickness showed that this property had no significant difference among developed nanocomposite films based on the CCD, indicating that the process of elaboration resulted in homogenous films. Moreover, a T-test was applied to compare thickness mean value of nanocomposite films (0.140 ± 0.02 mm) and control film (0.098 ± 0.01 mm), showing a significant difference ($p < 0.05$) among them.

This difference resulted from the incorporation of both antimicrobials, ZnO nanoparticles and pediocin, in the polymeric matrix. Previous works have indicated the modification of thickness caused by incorporation of ZnO nanoparticles and pediocin to a polymeric matrix (Li, Xing, Li, Jiang, & Ding, 2010; Santiago-Silva et al., 2009; Seo, Jeon, Jang, Bahadar Khan, & Han, 2011).

Mechanical properties of films are important characteristics for food packaging materials. They measure stretchability prior to breakage and film strength. In this way, the mechanical performance of developed nanocomposite films was studied by determining the tensile strength at break (MPa), load at break (N) and elongation at break (%).

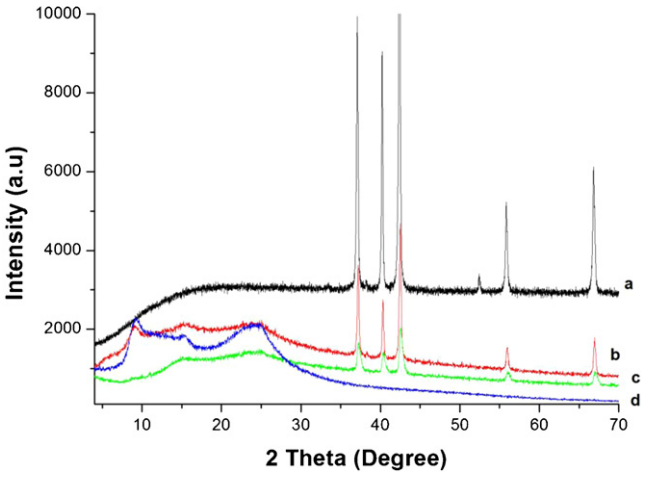

Fig. 1. XRD patterns of (a) pure ZnO nanoparticles, (b) 19.5% ZnO and 33% PED (TRT 6), (c) 11% ZnO and 50% PED (TRT 8), and (d) MC control film.

Load at break and tensile strength at break did not present significant differences among developed nanocomposite films. Also, the mean values of load at break (148.22 ± 20.69 N) and tensile strength at break (44.14 ± 6.89 MPa) of nanocomposite films were not significant different ($p > 0.05$) from mean values of control film (126.67 ± 25.65 N and 46.43 ± 4.47 MPa). These results indicated that the mechanical resistance of MC films was not affected after incorporation of ZnO nanoparticles and pediocin.

According to Bastarrachea, Dhawan, and Sablani (2011), a significant effect in the tensile properties is not expected when the molar mass of the antimicrobial molecule is smaller than the molar mass of the polymeric material. In this case, the molar mass of ZnO is 81.408 g/mol and the molar mass of pediocin is 4,629 g/mol, while the molar mass of MC is much higher, varying from 14,000 to 88,000 g/mol depending on its degree of substitution. Bastarrachea et al. (2011) indicated that the incorporation of the antimicrobial should not alter the conformation of the packaging material's polymer structure, thereby not influencing its tensile properties.

On the other hand, the regression model of elongation at break presented statistical significance among developed nanocomposite films, with a non-significant lack of fit (Table 2). The elongation at break of nanocomposite films was influenced by the linear effect of ZnO nanoparticles and pediocin, as well as by the quadratic effect of ZnO nanoparticles ($p < 0.05$) according to the analysis of regression coefficients of the response function.

The linear regression coefficient of ZnO nanoparticles was negative, indicating that a lower concentration of this antimicrobial allows more elongation of nanocomposite films. The linear regression coefficient of pediocin, which is positive, indicates that higher concentrations of this bioactive peptide result in higher values of elongation at break of nanocomposite films. Moreover, the significant quadratic coefficient of ZnO nanoparticles indicates that the elongation at break of nanocomposite films decreases quadratically when the concentration of ZnO increases (Fig. 2).

Results of elongation at break regarding ZnO concentration are in agreement with Li, Xing, Jiang, Ding, and Li (2009), who indicated the reverse effect of ZnO nanoparticles in the flexibility of the films. Moreover, the addition of pediocin resulted in increased values of elongation at break, indicating that this bioactive peptide acted as a plasticizer in the cellulosic matrix. This result is related to XRD patterns, which showed that higher concentration of pediocin resulted in diminished crystallinity of nanocomposite films.

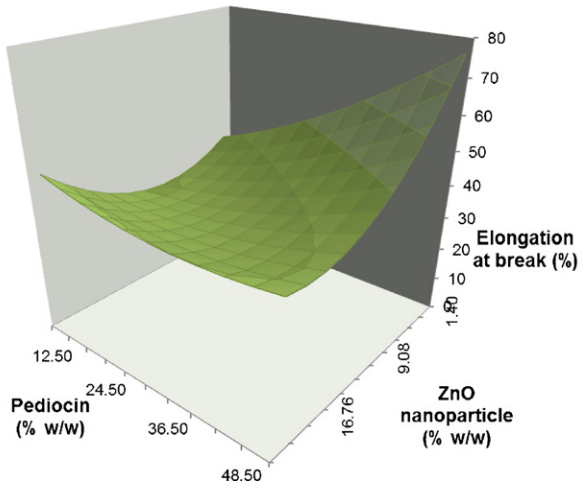

Fig. 2. Response surface of elongation at break (%) as a function of pediocin (%, w/w) and ZnO nanoparticles (%, w/w).

On the other hand, the elongation at rupture of packaging materials is inversely related to tensile strength, and a decrease in the values of load at break and tensile strength at break of developed nanocomposite films was expected. However, mechanical resistance of nanocomposite films, measured as load at break and tensile strength at break, presented no difference when compared to control film. This is probably because ZnO incorporation prevented the decrease of mechanical resistance after pediocin incorporation, since previous works have indicated that the incorporation of ZnO nanoparticles can enhance the strength but not the flexibility of nanocomposite films (Ma, Chang, Yang, & Yu, 2009).

3.3. Surface color measurement

The color of food packaging is an important factor in terms of general appearance and consumer acceptance (Bourtoom & Chinnan, 2008; Srinivasa, Ramesh, Kumar, & Tharanathan, 2003). The addition of active compounds that structurally bind with film forming solutions, could change the native color of the film (Rhim, Gennadios, Handa, Weller, & Hanna, 2000). In this way, the color of control film was transparent, while nanocomposite films incorporated with different concentrations of ZnO and pediocin presented a yellowish and whitish color.

Moreover, statistical analysis showed that the regression model for the colorimetric parameters L^*, b^*, total color difference (ΔE), opacity (OP), yellowness index (YI E313) and whiteness index (WI E313) presented significance differences among nanocomposite films, with a non-significant lack of fit (Table 2).

The colorimetric parameter L^* was influenced by the linear effect of pediocin ($p < 0.05$), while the addition of ZnO nanoparticles in tested conditions had no effect on this parameter. The linear regression coefficient of pediocin was negative, indicating that when higher concentrations of this bioactive peptide are incorporated, the luminosity of nanocomposite films is significantly diminished (Fig. 3a).

Also, the colorimetric parameter b^* was influenced by the linear effect of ZnO nanoparticles and pediocin ($p < 0.05$) according to the analysis of regression coefficients of the response function. Positive values of this parameter indicate a trend in the yellow direction and negative values indicate a trend in the blue direction. In this case, the linear regression coefficient of both antimicrobials affected the colorimetric parameter b^*, with the coefficient of ZnO nanoparticles being negative, indicating that higher concentrations of ZnO nanoparticles result in lower values of b^*. The coefficient of pediocin was positive, indicating that higher concentration of pediocin allows higher values of b^* (Fig. 3b).

On the other hand, the colorimetric parameter a^* made no significant difference to the developed nanocomposite films. This is probably due to the color that this coordinate represents, which are green, when negative values are obtained, or red, when positive values are obtained.

Moreover, the opacity (OP) of developed nanocoposite films was affected by the linear effect of ZnO nanoparticles and pediocin, indicating that increased concentrations of both antimicrobials results in increased values of OP. However, the quadratic and negative effect of ZnO indicates that the OP increase until certain ZnO concentration, and after reaching this critical concentration this parameter decreased quadratically (Fig. 3c).

Total color difference (ΔE) was affected by the linear and negative effect of ZnO and the positive linear effect of pediocin, indicating that high concentrations of ZnO results in low values of ΔE while high concentrations of pediocin results in high values of this colorimetric parameter (Fig. 3d).

As expected, whiteness index (WI E313) of nanocomposite films was affected by linear effect of both antimicrobials; nevertheless pediocin presented a negative coefficient indicating that high concentrations of pediocin results in lower values of this index (Fig. 3e).

Moreover, yellowness index (YI E313) was affected by the addition of pediocin, since this antimicrobial in the form of concentrated powder presents naturally a yellow color and the presence of ZnO did not have influence on this parameter (Fig. 3f). Similar to our results, Chandramouleeswaran et al. (2007) developed ZnO–polypropylene (PP) nanocomposites and indicated that the whitening effect on PP is due to the presence of ZnO nanoparticles.

Moreover, similar to pediocin other bacteriocins have shown similar effects on color parameters after incorporation in polymeric matrixes. In this way, alginate and PVOH films showed a significant decrease of L^* values (lightness) and an increase of b^* values (yellowness) due to enterocin incorporation, a bacteriocin produced by *Enterococcus faecium* CTC492 isolated from meat products (Marcos, Aymerich, Monfort, & Garriga, 2010). Also, the incorporation of nisin, a bacteriocin produced by certain strains of *Lactococcus lactis*, in tapioca starch films and its mixtures with hydroxypropyl methylcellulose resulted in a decrease of L^* values and increase of b^* and YI values compared to control films (Basch et al., 2012). The authors attributed the yellowish trend of the films to the own color of nisin.

Thus, based on our results and related works, the presence of pediocin in the formulation of developed nanocomposite films produced slightly yellowish films; however, this effect was balanced by the incorporation of ZnO nanoparticle, resulting in a whitish coloration.

3.4. Microscopy characterization

Morphological analyses by scanning electron microscopy (SEM) of MC film (control film) showed a homogeneous surface, with the presence of scarce undissolved polymeric resin. Moreover, nanocomposite films showed the presence of ZnO nanoparticles. The addition of pediocin in high concentrations resulted in the formation of crater-like pits (Fig. 4a–c).

The formation of crater-like pits as an effect of pediocin was verified by the elaboration and SEM analysis of a MC film incorporated only with the maximum concentration of pediocin (50%, w/w) tested in this work. Also, the MC film incorporated only with 20% (w/w) of ZnO nanoparticles was observed in the SEM for comparison (Supplementary Fig. 1a and b).

Supplementary data associated with this article can be found, in the online version, at http://dx.doi.org/10.1016/j.carbpol.2013.01.003.

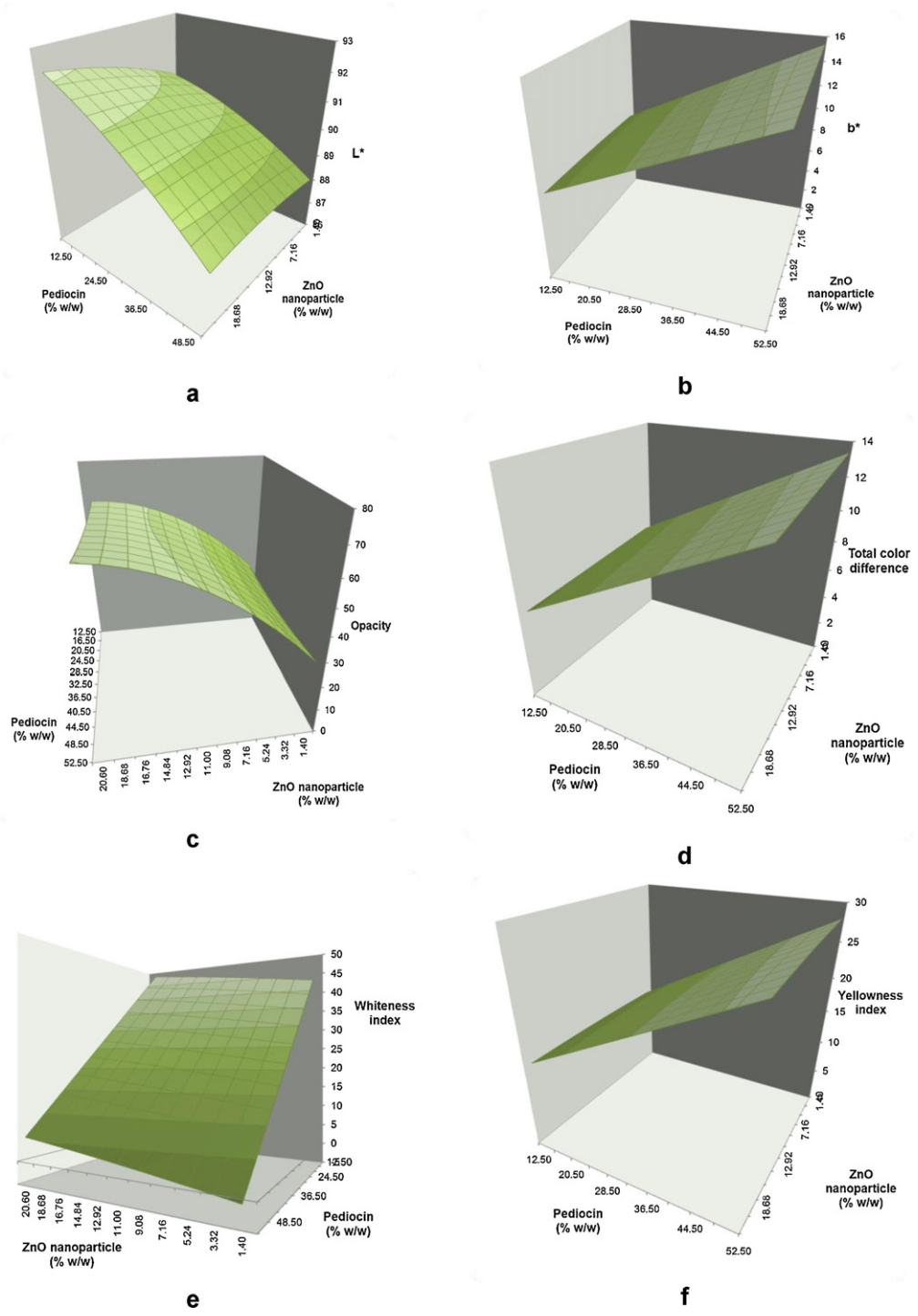

Fig. 3. Response surface of the colorimetric parameters: (a) L^*, (b) b^*, (c) opacity, (d) total color difference, (e) whiteness index, and (f) yellowness index as a function of pediocin (%, w/w) and ZnO nanoparticles (%, w/w).

A high number of crater-like pits were observed in the surface of the film with 50% pediocin, presenting a sponge-like and loosely filled structure. The greater formation of crater-like pits revealed a weak interaction of the polymeric matrix, which failed to retain microscopic surface integrity. Moreover, images of nanocomposite films showed ZnO nanoparticles trapped in crater-like pits created by pediocin (Supplementary Fig. 1c). This probably caused the lack of improvement of mechanical resistance of nanocomposite films after ZnO incorporation, as observed for load at break and tensile strength.

In addition, atomic force microscopy (AFM) presented 3D topographic images of nanocomposite film surfaces (Fig. 4d–f). These images confirmed the results observed by SEM, showing the formation of crater-like pits in nanocomposite films. These crater-like pits are clearly observed in image of treatment 8 (Fig. 4b), where the concentration of pediocin was considerably higher than the concentration of ZnO. On the other hand, the control film had a very homogeneous surface with few points of undissolved polymeric resin, as observed in the SEM microphotograph. The crater-like pits, as observed in the nanocomposite films, were not observed in the

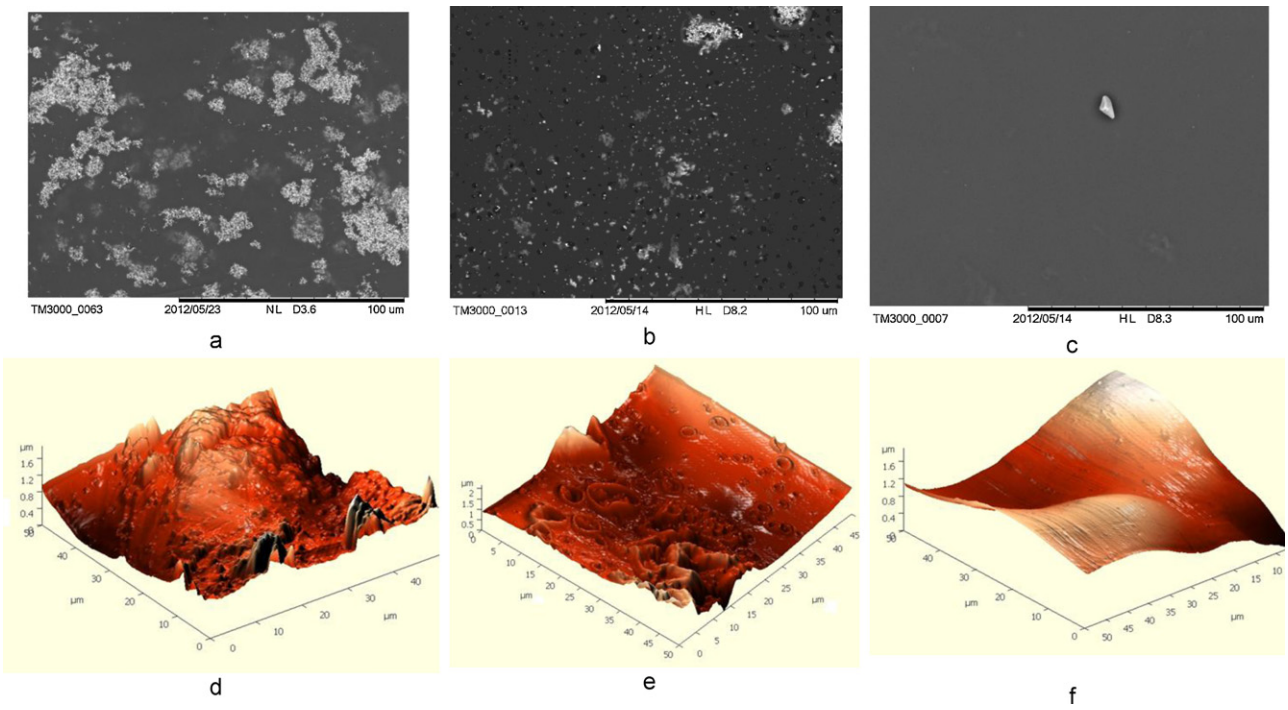

Fig. 4. SEM photomicrograph of nanocomposite films incorporated with (a) 19.5% ZnO and 33% PED (TRT6), (b) 11% ZnO and 50% PED (TRT8), (c) control film; and AFM photomicrograph of nanocomposite films incorporated with (d) 19.5% ZnO and 33% PED (TRT6), (e) 11% ZnO and 50% PED (TRT8), (f) control film. SEM images at 1000× magnification.

control film, indicating that these cavities form as a result of the addition of pediocin.

In order to prove our theory about the formation of the crater-like pits, we used AFM to analyze the surface of MC film incorporated only with the highest concentration of pediocin (50%, w/w) or ZnO nanoparticles (20%, w/w) used in this study (Supplementary Fig. 1d and e). In agreement with the SEM images, AFM showed the formation of crater-like pits created by pediocin.

Espinoza-Herrera et al. (2011) indicated that the formation of crater-like pits, also known as pores, in the cellulosic polymeric matrix is probably due to a smaller transference of mass, related to solvent evaporation, and consequently a slower drying speed. Particularly in this work, it is probable that polysaccharides that constitute the matrix film are bonded to pediocin and form a more compact structure that reduce the transference rate of solvent (in this case water) from the film forming solution, leading to the formation of crater-like pits and consequently to a rougher surface. These results are related to the results obtained by XRD, which showed that increased pediocin concentration resulted in diminished crystallinity of nanocomposite films.

3.5. Swelling tests

The sensitivity of developed nanocomposite films to water was investigated by means of their swelling degree. Swelling degree is an important parameter in order to know the stability and quality changes of packaging materials during packaging and storage of food product (Abdollahi, Rezaei, & Farzi, 2012; Srinivasa, Ramesh, & Tharanathan, 2007).

Results of the swelling test showed that this property had no significant difference among developed nanocomposite films according to the CCD. However, when the *T*-test was applied, a significant difference ($p < 0.05$) was observed among the mean value of swelling degree of nanocomposite films (16.4 ± 2.1 g of H_2O/g of film) and control film (21.3 ± 3.2 g of H_2O/g of film), indicating that the control film absorbed large amounts of water compared to developed nanocomposite films. To prove adequate barrier properties, films must exhibit low swelling ability (Guiga et al., 2010; Jipa et al., 2012); therefore this is a promising result.

We attribute the reduction of swelling degree of nanoacomposite films to the presence of ZnO nanoparticles in MC matrix since, although the incorporation of pediocin in the MC matrix resulted in the formation of crater-like pits, ZnO nanoparticles exhibited good intercalation in the MC matrix, as observed in the AFM images, which avoided the absorption of water.

Studies are scarce regarding the effect of ZnO nanoparticles on the swelling degree of nanocomposite films. However, Liu and Kim (2012) reported that ZnO nanoparticles have previously been shown to diminish the swelling degree of nanocomposites. In this way, they have indicated that the incorporation of ZnO and silver nanoparticles in genipin-crosslinked chitosan nanocomposites leads to decreased swelling compared to control film.

3.6. Thermogravimetric analysis

Determining the thermal resistance allows studying structural changes caused by temperature variations on packaging (Espitia et al., 2012). The thermal stability of developed nanocomposite films was investigated by means of thermogravimetric analysis (Fig. 5).

The presence of pediocin caused a lower film decomposition starting temperature. In this way, the nanocomposite film with 50% of pediocin (TRT 8) presented a starting thermal decomposition at 438 °C and nanocomposite film with 33% of pediocin (TRT 6) presented this at 478 °C, while the control film (with no pediocin) presented the highest starting decomposition temperature, 510 °C.

However, the temperature value at the maximum decomposition rate, obtained from the derivative thermogravimetric (DTG) curves, of nanocomposite film with the highest concentration of ZnO (TRT 6) was 458 °C, higher when compared to the temperature of control film (450 °C) or to the temperature of nanocomposite film with 11% of ZnO and 50% of pediocin (438 °C). Thus, the

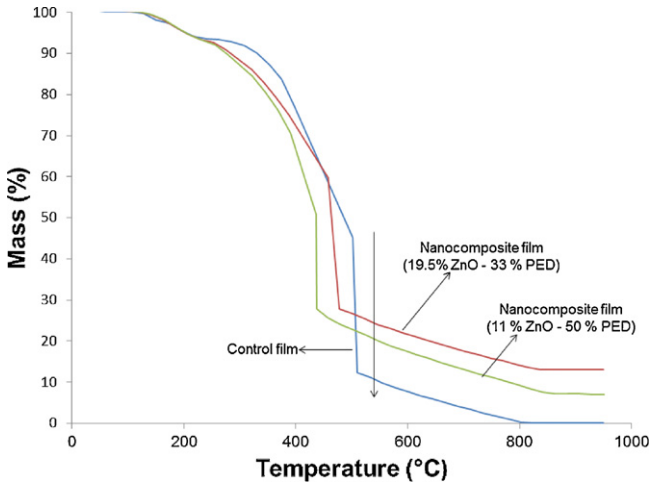

Fig. 5. TGA curve of nanocomposite films with highest concentration of ZnO nanoparticles (TRT6: 19.5% ZnO; 33% PED), highest concentration of pediocin (TRT8: 11% ZnO; 50% PED) and control film.

nanocomposite film with a high concentration of ZnO nanoparticles showed enhanced thermal stability in comparison with control film and nancomposite film with high concentration of pediocin.

Similar to our results, Yu, Yang, Liu, and Ma (2009) reported that the decomposed temperature of carboxymethylcellulose (CMC) sodium nanocomposites with ZnO nanoparticles was 295.4 °C, while the control was 293.7 °C, indicating that ZnO–CMC nanocomposite film exhibited better thermal stability than control CMC film. They ascribed this result to the interaction between ZnO and CMC.

Moreover, our results are in agreement with XRD analysis, which indicated that the presence of ZnO nanoparticles affected MC crystallinity, resulting in narrows peaks. Vicentini, Smania, and Laranjeira (2010) reported similar results, indicating that the thermal resistance improvement of biopolymer films by ZnO is due to a decrease in the interatomic distances, and therefore more energy is being required to decompose these films.

Moreover, the nanocomposite film incorporated with the high pediocin concentration showed the lowest thermal resistance, presenting the lowest thermal decomposition starting temperature as well as the lowest temperature at which the maximum decomposition rate is achieved.

This result is probably due to the organic nature of pediocin. Pediocin is a heat-stable peptide, and its antimicrobial activity is retained at 100 °C, but reduced at 121 °C (Bhunia, Johnson, & Ray, 1988; Rodríguez et al., 2002), presenting thermal decomposition above this temperature range.

Moreover, a total weight loss was observed in control film (99.71%), as expected, while nanocomposite films with ZnO nanoparticles lost less weight (86.98% for TRT 6 and 92.92% for TRT 8). Diminished weight loss was observed with increasing concentrations of ZnO nanoparticles incorporated in the film. This is attributed to the amount of ZnO nanoparticles deposited on each nanocomposite film.

3.7. Antimicrobial activity assay

Developed nanocomposite films presented antimicrobial activity against tested microorganisms, *L. monocytogenes* and *S. aureus* (Fig. 6). However, nanocomposite films had no significant difference among treatments. The average values of the measured inhibition zone around each disc of films (cm) were calculated for each microorganism. The average inhibition zone for *L. monocytogenes* was 2 ± 0.1 cm, while for *S. aureus* was 1.6 ± 0.2 cm.

Antimicrobial activity *in vitro* of ZnO nanoparticles against Gram-positive bacteria, such as *S. aureus*, has been previously reported (Adams, Lyon, & Alvarez, 2006; Premanathan, Karthikeyan, Jeyasubramanian, & Manivannan, 2011; Reddy et al., 2007). Moreover, studies have indicated the antimicrobial activity of ZnO nanoparticles when incorporated in polymeric matrixes. Li et al. (2009) observed that the growth of *S. aureus* was affected significantly by ZnO-coated films compared to control film. Also, Nafchi, Alias, Mahmud, & Robal (2012) indicated that ZnO nanoparticles (rod shape) incorporated in sago starch films exhibited excellent antimicrobial activity against *S. aureus*.

Although studies regarding antimicrobial activity of ZnO nanoparticles against *L. monocytongenes* are limited, Jin, Sun, Su, Zhang, and Sue (2009) have indicated that ZnO nanoparticles suspended in polyvinylprolidone (PVP) gel resulted in a 5.3 log reduction of *L. monocytogenes*, showing significant antimicrobial activities in growth media.

Moreover, pediocin is a bioactive peptide with high specific activity against *L. monocytogenes*, and the potential of this bioactive peptide in food packaging application has been reported (Coma, 2008; Santiago-Silva et al., 2009). In addition, *in vitro* studies indicate that pediocin is adsorbed to Gram-positive bacteria, including *S. aureus*, which results in cell death (Bhunia et al., 1988; Bhunia, Johnson, Ray, & Kalchayanand, 1991). Thus, developed nanocomposite films incorporated with ZnO nanoparticles and pediocin

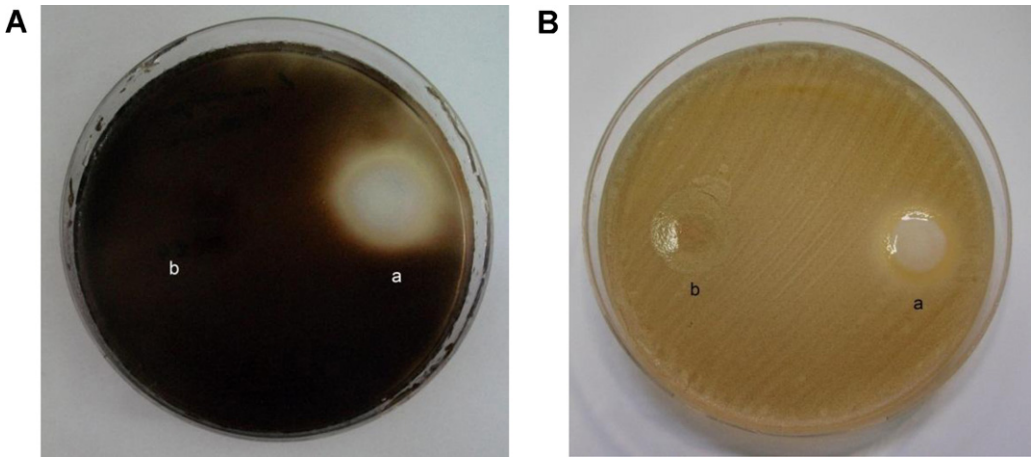

Fig. 6. Antimicrobial activity of nanocomposite films: (a) incorporated with ZnO nanoparticles (17%, w/w) and pediocin (20%, w/w) and (b) control film against *L. monocytogenes* (A) and *S. aureus* (B).

have potential to be used for controlling *S. aureus* and *L. monocytogenes* in food preservation.

3.8. Optimization by the desirability function approach

Elongation at break and colorimetric parameters L^*, b^*, OP, YI and WI of developed films were selected for simultaneous optimization by the desirability approach. The optimization was performed in order to achieve films with good mechanical and colorimetric properties. Other responses were not considered in this analysis since they presented no statistical significance according to the RSM.

The optimization showed that films with desired characteristics can be obtained incorporating 20% (w/w) ZnO nanoparticles and 15% (w/w) pediocin (Supplementary Fig. 2).

Supplementary data associated with this article can be found, in the online version, at http://dx.doi.org/10.1016/j.carbpol.2013.01.003.

4. Conclusions

The use of natural antimicrobial agents, such as pediocin, associated to nanotechnology allowed the development of new antimicrobial packaging for food preservation. In this experiment, methyl cellulose was used as a polymeric matrix due to its biodegradability, large availability in nature, low cost and easy processing.

Results from XRD showed that the addition of ZnO nanoparticles and pediocin affected the crystallinity of methyl cellulose matrix. Mechanical resistance of nanocomposite films, measured as load at break and tensile strength at break, did not present significant differences among films. However, elongation at break presented statistical significance, indicating that ZnO incorporation resulted in more rigid films, while the addition of pediocin resulted in increased values of elongation at break. The presence of pediocin in nanocomposite films produced slightly yellowish films. However, this effect was balanced by the incorporation of ZnO nanoparticles, resulting in a whitish coloration.

SEM and AFM images showed that ZnO nanoparticles exhibited good intercalation in MC matrix and the addition of pediocin in high concentrations resulted in the formation of crater-like pits in nanocomposite film surface. The swelling degree of nanocomposite films was significantly diminished compared to control due to ZnO nanoparticles. Also, incorporation of ZnO in higher concentration allowed enhanced thermal stability when compared to control and nancomposite film with high concentration of pediocin.

Developed nanocomposite films presented antimicrobial activity against *L. monocytogenes* and *S. aureus*.

Based on the results of the desirability function analysis, optimal concentrations of tested antimicrobials are 20% (w/w) ZnO nanoparticles and 15% (w/w) pediocin. The results of this research indicated the potential use of developed nanocomposite films for the control of these food borne pathogens. Finally, more studies are needed to test the antimicrobial activity of developed nanocomposite films on food matrixes.

Acknowledgments

The authors thank Mr. Nicholas J. Walker for providing language help and writing assistance, Professor Maurício P.F. Fontes for the XRD analysis and Professor Angélica C.O Carneiro for TGA analysis. The authors gratefully acknowledge the financial support for this research provided by a doctoral scholarship from Coordenação de Aperfeiçoamento de Pessoal de Nível Superior (CAPES) and a grant from Conselho Nacional de Desenvolvimento Científico e Tecnológico (CNPq).

References

Abdollahi, M., Rezaei, M., & Farzi, G. (2012). A novel active bionanocomposite film incorporating rosemary essential oil and nanoclay into chitosan. *Journal of Food Engineering*, *111*(2), 343–350.

Adams, L. K., Lyon, D. Y., & Alvarez, P. J. J. (2006). Comparative eco-toxicity of nanoscale TiO_2, SiO_2, and ZnO water suspensions. *Water Research*, *40*(19), 3527–3532.

Arora, A., & Padua, G. W. (2010). Review: Nanocomposites in food packaging. *Journal of Food Science*, *75*(1), R43–R49.

ASTM. (2008). *ASTM E308-08 Standard practice for computing the colors of objects by using the CIE system*. West Conshohocken, PA: ASTM International.

ASTM. (2009). *ASTM D 882-09 Standard test method for tensile properties of thin plastic sheeting*. West Conshohocken, PA: ASTM International.

ASTM. (2010). *ASTM E313-10 Standard practice for calculating yellowness and whiteness indices from instrumentally measured color coordinates*. West Conshohocken, PA: ASTM International.

Basch, C., Jagus, R., & Flores, S. (2012). Physical and antimicrobial properties of tapioca starch-HPMC edible films incorporated with nisin and/or potassium sorbate. *Food and Bioprocess Technology*, 1–10. http://dx.doi.org/10.1007/s11947-012-0860-3

Bastarrachea, L., Dhawan, S., & Sablani, S. (2011). Engineering properties of polymeric-based antimicrobial films for food packaging: A review. *Food Engineering Reviews*, *3*(2), 79–93.

Bhunia, A. K., Johnson, M. C., & Ray, B. (1988). Purification, characterization and antimicrobial spectrum of a bacteriocin produced by *Pediococcus acidilactici*. *Journal of Applied Microbiology*, *65*(4), 261–268.

Bhunia, A. K., Johnson, M. C., Ray, B., & Kalchayanand, N. (1991). Mode of action of pediocin AcH from *Pediococcus acidilactici* H on sensitive bacterial strains. *Journal of Applied Microbiology*, *70*(1), 25–33.

Bourtoom, T., & Chinnan, M. S. (2008). Preparation and properties of rice starch–chitosan blend biodegradable film. *LWT—Food Science and Technology*, *41*(9), 1633–1641.

Chandramouleeswaran, S., Mhaske, S. T., Kathe, A. A., Varadarajan, P. V., Prasad, V., & Vigneshwaran, N. (2007). Functional behaviour of polypropylene/ZnO—soluble starch nanocomposites. *Nanotechnology*, *18*(385702), 8 pp.

Coma, V. (2008). Bioactive packaging technologies for extended shelf life of meat-based products. *Meat Science*, *78*(1–2), 90–103.

Derringer, G., & Suich, R. (1980). Simultaneous optimization of several response variables. *Journal of Quality Technology*, *12*(4), 214–219.

EPA. (2011). *Municipal solid waste*. Retrieved from http://www.epa.gov/osw/nonhaz/municipal/index.htm

Espinoza-Herrera, N., Pedroza-Islas, R., San Martín-Martinez, E., Cruz-Orea, A., & Tomás, S. (2011). Thermal, mechanical and microstructures properties of cellulose derivatives films: A comparative study. *Food Biophysics*, *6*(1), 106–114.

Espitia, P., Soares, N. d. F., Coimbra, J. S. d. R., Andrade, N. J., Cruz, R. S., & Medeiros, E. A. A. (2012). Zinc oxide nanoparticles: Synthesis, antimicrobial activity and food packaging applications. *Food and Bioprocess Technology*, *5*(5), 1447–1464.

FDA. (2011). *Part 182—Substances generally recognized as safe*. Retrieved from http://ecfr.gpoaccess.gov/cgi/t/text/text-idx?c=ecfr&sid=786bafc6f6343634fbf79fcdca7061e1&rgn=div5&view=text&node=21:3.0.1.1.13&idno=21#21:3.0.1.1.13.9

Guiga, W., Swesi, Y., Galland, S., Peyrol, E., Degraeve, P., & Sebti, I. (2010). Innovative multilayer antimicrobial films made with Nisaplin® or nisin and cellulosic ethers: Physico-chemical characterization, bioactivity and nisin desorption kinetics. *Innovative Food Science and Emerging Technologies*, *11*(2), 352–360.

Jin, T., Sun, D., Su, J. Y., Zhang, H., & Sue, H. J. (2009). Antimicrobial efficacy of zinc oxide quantum dots against *Listeria monocytogenes*, *Salmonella enteritidis*, and *Escherichia coli* O157:H7. *Journal of Food Science*, *74*(1), M46–M52.

Jipa, I. M., Stoica-Guzun, A., & Stroescu, M. (2012). Controlled release of sorbic acid from bacterial cellulose based mono and multilayer antimicrobial films. *LWT—Food Science and Technology*, *47*(2), 400–406.

Lagarón, J. M., & Fendler, A. (2009). High water barrier nanobiocomposites of methyl cellulose and chitosan for film and coating applications. *Journal of Plastic Film and Sheeting*, *25*(1), 47–59.

Li, X., Xing, Y., Jiang, Y., Ding, Y., & Li, W. (2009). Antimicrobial activities of ZnO powder-coated PVC film to inactivate food pathogens. *International Journal of Food Science & Technology*, *44*(11), 2161–2168.

Li, X., Xing, Y., Li, W., Jiang, Y., & Ding, Y. (2010). Antibacterial and physical properties of poly(vinyl chloride)-based film coated with ZnO nanoparticles. *Food Science and Technology International*, *16*(3), 225–232.

Liu, Y., & Kim, H.-I. (2012). Characterization and antibacterial properties of genipin-crosslinked chitosan/poly(ethylene glycol)/ZnO/Ag nanocomposites. *Carbohydrate Polymers*, *89*(1), 111–116.

Ma, X., Chang, P. R., Yang, J., & Yu, J. (2009). Preparation and properties of glycerol plasticized-pea starch/zinc oxide-starch bionanocomposites. *Carbohydrate Polymers*, *75*(3), 472–478.

Marcos, B., Aymerich, T., Monfort, J. M., & Garriga, M. (2010). Physical performance of biodegradable films intended for antimicrobial food packaging. *Journal of Food Science*, *75*(8), E502–E507.

Nafchi, A. M., Alias, A. K., Mahmud, S., & Robal, M. (2012). Antimicrobial, rheological, and physicochemical properties of sago starch films filled with nanorod-rich zinc oxide. *Journal of Food Engineering*, *113*(4), 511–519.

Premanathan, M., Karthikeyan, K., Jeyasubramanian, K., & Manivannan, G. (2011). Selective toxicity of ZnO nanoparticles toward Gram-positive bacteria and cancer cells by apoptosis through lipid peroxidation. *Nanomedicine: Nanotechnology, Biology and Medicine*, *7*(2), 184–192.

Reddy, K. M., Feris, K., Bell, J., Wingett, D. G., Hanley, C., & Punnoose, A. (2007). Selective toxicity of zinc oxide nanoparticles to prokaryotic and eukaryotic systems. *Applied Physics Letters*, *90*(21), 213902.

Rhim, J. W., Gennadios, A., Handa, A., Weller, C. L., & Hanna, M. A. (2000). Solubility, tensile, and color properties of modified soy protein isolate films. *Journal of Agricultural and Food Chemistry*, *48*(10), 4937–4941.

Rimdusit, S., Jingjid, S., Damrongsakkul, S., Tiptipakorn, S., & Takeichi, T. (2008). Biodegradability and property characterizations of methyl cellulose: Effect of nanocompositing and chemical crosslinking. *Carbohydrate Polymers*, *72*(3), 444–455.

Rodríguez, J. M., Martínez, M. I., & Kok, J. (2002). Pediocin PA-1, a wide-spectrum bacteriocin from lactic acid bacteria. *Critical Reviews in Food Science and Nutrition*, *42*(2), 91–121.

Santiago-Silva, P., Soares, N. F. F., Nóbrega, J. E., Júnior, M. A. W., Barbosa, K. B. F., Volp, A. C. P., & Würlitzer, N. J. (2009). Antimicrobial efficiency of film incorporated with pediocin (ALTA® 2351) on preservation of sliced ham. *Food Control*, *20*(1), 85–89.

Seo, J., Jeon, G., Jang, E. S., Bahadar Khan, S., & Han, H. (2011). Preparation and properties of poly(propylene carbonate) and nanosized ZnO composite films for packaging applications. *Journal of Applied Polymer Science*, *122*(2), 1101–1108.

Soares, N. F. F., Pires, A. C. S., Camilloto, G. P., Santiago-Silva, P., Espitia, P. J. P., & Silva, W. A. (2009). Recent patents on active packaging for food application. *Recent Patents on Food, Nutrition & Agriculture*, *1*(1), 171–178.

Srinivasa, P. C., Ramesh, M. N., Kumar, K. R., & Tharanathan, R. N. (2003). Properties and sorption studies of chitosan–polyvinyl alcohol blend films. *Carbohydrate Polymers*, *53*(4), 431–438.

Srinivasa, P. C., Ramesh, M. N., & Tharanathan, R. N. (2007). Effect of plasticizers and fatty acids on mechanical and permeability characteristics of chitosan films. *Food Hydrocolloids*, *21*(7), 1113–1122.

Teófilo, R. F., & Ferreira, M. M. C. (2006). Quimiometria II: planilhas eletrônicas para cálculos de planejamentos experimentais, um tutorial. *Química Nova*, *29*, 338–350.

Tunç, S., & Duman, O. (2011). Preparation of active antimicrobial methyl cellulose/carvacrol/montmorillonite nanocomposite films and investigation of carvacrol release. *LWT—Food Science and Technology*, *44*(2), 465–472.

Vicentini, D. S., Smania, A., Jr., & Laranjeira, M. C. M. (2010). Chitosan/poly (vinyl alcohol) films containing ZnO nanoparticles and plasticizers. *Materials Science and Engineering: C*, *30*(4), 503–508.

Yu, J., Yang, J., Liu, B., & Ma, X. (2009). Preparation and characterization of glycerol plasticized-pea starch/ZnO–carboxymethylcellulose sodium nanocomposites. *Bioresource Technology*, *100*(11), 2832–2841.